Electronic interaction of very slow light ions in Au: Electronic stopping and electron emission

S. N. Markin,[1] D. Primetzhofer,[1] S. Prusa,[2] M. Brunmayr,[3] G. Kowarik,[3] F. Aumayr,[3] and P. Bauer[1]
[1]*Institut für Experimentalphysik, Abteilung Atom- und Oberflächenphysik, Johannes Kepler Universität, Altenbergerstrasse 69, A-4040 Linz, Austria*
[2]*Institute of Physical Engineering, Brno University of Technology, Technická 2, Brno 61669, Czech Republic*
[3]*Institut für Allgemeine Physik, TU Wien, Wiedner Hauptstrasse 8-10, 1040 Vienna, Austria*
(Received 30 May 2008; revised manuscript received 30 September 2008; published 25 November 2008)

Electronic stopping and ion-induced electron emission during the interaction of slow ($v<0.1$ a.u.) H^+ and D^+ ions with polycrystalline Au targets have been investigated. Electronic stopping is deduced from time-of-flight low-energy ion scattering measurements in backscattering geometry using polycrystalline films of several nanometers thick. Current measurements are performed to determine the ion-induced electron emission yield. Both in electronic stopping and in ion-induced electron emission we find a rather sharp, distinctive threshold velocity of ~0.19 a.u. for specific excitation and emission of 5*d* electrons. Below this threshold the projectiles interact exclusively with the 6*s* electrons.

DOI: 10.1103/PhysRevB.78.195122 PACS number(s): 34.50.Fa, 79.20.Rf

I. INTRODUCTION

Electronic interactions of slow ions, such as electronic stopping and ion-induced electron emission, are of fundamental interest. A profound understanding of electronic excitation in metals by slow light ions is important for two reasons: first, to refine the theoretical models describing the ion-atom interaction in this velocity range and second, to permit further development of analytical techniques for quantitative surface analysis, e.g., low-energy ion scattering (LEIS). Ions with velocities smaller than the Fermi velocity of a solid ($v<v_F$) can excite electron-hole pairs only via binary collisions with electrons in the valence or conduction band. Therefore, the band structure of a metal is expected to have a significant influence on the electronic interactions of a slow projectile.

Inelastic processes of ions in solids have been intensively studied in the range of velocities $v>v_F$. In the velocity range below the stopping maximum the ion-electron interaction is so strong that linear theories brake down and only nonperturbative models can be considered as potentially adequate.[1] For instance, density-functional theory (DFT) has been applied to describe nonlinear effects in the energy loss of slow ions in a free-electron gas (FEG).[2–6] At low velocities, a projectile of atomic number Z_1 experiences an energy loss $-dE$ in a FEG of a finite thickness dx, that is given by the stopping power $S=-dE/dx$, which is proportional to the velocity

$$S = Q(Z_1, r_s)v. \tag{1}$$

The proportionality constant, i.e., the "friction coefficient" Q, depends on Z_1 and the density parameter $r_s=[3/(4\pi n_e)]^{1/3}$, with the electron density n_e. Any deviation from velocity proportional stopping is accounted for by a velocity dependence of Q. In many cases the stopping cross section ε is the relevant quantity; ε is related to S via $\varepsilon=S/n$, with n being the atomic density.

A velocity threshold was observed in the electronic energy loss of H projectiles in a polycrystalline Au film in backscattering[7,8] as well as in transmission through single crystals in channeling geometry.[9] The latter data were compared to DFT calculations accounting for the spatial distribution of *sp* and *d* electrons. The localized *d* electrons are found responsible for the appearance of the threshold. Note that the resulting energy-loss data are not directly comparable since different impact-parameter selection has to be expected in channeling geometry and in a random direction, but qualitatively speaking, the same type of threshold behavior for the interaction with the *d* electrons is expected in both types of experiments.

Electron ejection from Au due to the impact of protons is dominated by kinetic electron emission (KE) where the transfer of kinetic energy of the projectile leads to electronic excitations and electron emission.[10] Despite considerable efforts over the last decades toward a fundamental understanding of kinetic emission phenomena, basic features of this process are still a matter of debate.[11] In this respect we mention in particular the kinematic threshold behavior of KE, which seems to be directly related to the energy transfer in collisions between the atomic projectiles and electrons and the energy needed to overcome the vacuum-solid potential barrier (approximately work function W).

Considering only binary collisions between the proton and electrons of an idealized Fermi gas (Fermi energy E_F, Fermi velocity v_F) leads to a so-called "classical threshold" impact velocity v_{th} (Ref. 12):

$$v_{\mathrm{th}} = \frac{1}{2}v_F\left[\left(1+\frac{W}{E_F}\right)^{1/2}-1\right]. \tag{2}$$

Assuming a work function for the Au 6*s* electrons of about 5.1 eV (Ref. 13) and a Fermi energy of roughly 7.3 eV (Ref. 14) v_{th} is about 2.4×10^5 m/s or ca. 300 eV/amu.[15]

Irrespective of the fact that a variety of studies on atom or ion impact on metal targets are consistent with a kinematic threshold, in many cases evidence is reported for subthreshold electron emission, in general attributed to electron promotion mechanisms during impact of atomic projectiles on solid targets.[12,15,16] In this paper, we present an experimental proof for band-structure effects in ion-induced electron emission as a consequence of the finite energy needed to excite the 5*d* electrons in gold.

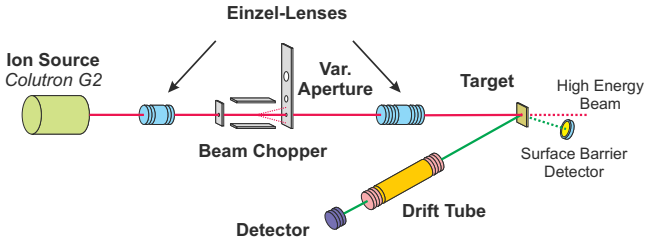

FIG. 1. (Color online) Schematic representation of the experimental setup ACOLISSA. Shown are the TOF beam lines before and after scattering off the surface of the target. Additionally, dotted lines indicate directions of incoming and outgoing high energy beam trajectories.

II. EXPERIMENT

A. Energy loss

The energy-loss experiments were performed in the setup ACOLISSA described in detail in Ref. 17. Here, just its main features are summarized. As shown in Fig. 1, a beam of monoenergetic ions is created in the ion source, passes through the chopper and a system of focusing einzel lenses, and is directed onto the target at a small angle α, measured with respect to the surface normal. Projectiles, backscattered by a large angle θ (fixed to 129°), are detected by use of a set of two channel plates in chevron configuration. Thus, a time-of-flight (TOF) spectrum is recorded. The TOF spectrum is converted to an energy spectrum by a standard procedure.

Two gold samples were produced by *in situ* evaporation in the analytical chamber (ANA) with a base pressure in the 10^{-10} mbar range, using a three-cell evaporator (OMICRON EFM 3T). As a substrate, a sputter-cleaned Si wafer with a B buffer layer on top was used. The thickness of the evaporated Au layer was controlled online by the flux monitor of the evaporator. After evaporation, the samples were transferred to the TOF-LEIS chamber without breaking the vacuum. In addition, one Au sample was prepared by *ex situ* evaporation with thickness control by a quartz microbalance. Since in both cases the thickness information is not quantitative, the thickness values were fixed to 4.6, 5.4, and 7.0 nm such that the resulting stopping cross section coincides with the value recommended by the (proton stopping and ranges) PSTAR compilation at 9 keV.[18] For one of the Au films homogeneity and thickness were analyzed by Auger-electron spectroscopy (AES) and TOF-LEIS.[19] Roughness and morphology of the Au layer were measured *ex situ* by atomic force microscopy (AFM, Veeco Instruments Dimension 3100) in the tapping mode,[20] yielding a rms surface roughness of 0.29 and 0.51 nm for B/Si and Au/B/Si, respectively.

The thickness of the Au films was small enough to assure that after being backscattered from the Au/B interface the projectiles could still leave the surface and be detected in the whole range of projectile energies. TOF-LEIS spectra were measured using H^+, H_2^+, H_3^+, D^+, D_2^+, and D_3^+ as projectiles, with energies in the range 0.167–9 keV/A (A denotes the relative atomic mass) and subsequently converted to energy spectra. In the spectra, projectiles scattered from Au atoms dominate, with a finite-energy width corresponding to the thickness of the Au layer, similarly as in Rutherford backscattering (RBS). Because of the high scattering probability at low energies, the detailed shapes of the spectra will be influenced by multiple scattering. Therefore, the safest way to deduce the electronic stopping cross section is to compare the experimental spectra to spectra obtained from Monte Carlo simulations (TRBS) (Ref. 21) as described below.

B. Electron emission

The electron emission yield measurements were performed with an experimental setup at the electron cyclotron resonance ion source at the TU Wien (for a description of the ion source see Ref. 22) The source is capable of producing singly and multiply charged ions of various species with acceleration voltages between 1 and 10 kV at electrical currents between 10 and 1000 nA depending on the species. The extracted ion beam is focused by two magnetic-quadrupole lenses with perpendicular focusing planes, mass separated by a magnetic sector field at an aperture of 3 mm diameter, which forms the entrance of the beam line. The ion beam can be decelerated and focused onto the target surface with a custom deceleration lens system, designed for voltages up to 1.5 kV, where an incidental particle flux of approximately 10^{12} cm^{-2} s^{-1} is maintained. Before each measurement, the solid polycrystalline Au sample is sputter cleaned by 2 keV Ar^+ ions in grazing incidence; subsequently the recipient pressure returns to a base pressure in the range of 10^{-10} mbar. The electron emission yield is deduced from the electrical currents[23] measured at the sample at a highly transparent grid and a collector electrode. The potentials of sample, grid, and collector are each digitally controlled and the electrical currents of grid and collector are measured simultaneously via separate standard electrometers. The switching of the electrodes' voltages as well as the corresponding current characteristics is illustrated schematically in Fig. 2. For extraction of the emitted electrons a voltage of +20 V is applied to the grid with respect to the sample. Complete suppression of the corresponding electron current is achieved by biasing the grid to −60 V with respect to the target. The collector is always kept 30 V more positive than the grid in order to suppress secondary electron emission from the collector electrode. The grid's transparency c was determined independently by calibration measurements (electron emission from gold by keV Ar^+ ions). A value of $c=0.90\pm0.03$ resulted.

Two different evaluation methods are used to determine the emission yield γ: (i) Using the target current only, one obtains $\gamma_1=q(\frac{I_T^+}{I_0}-1)$, with q being the projectile's charge state, I_T^+ denotes the target current when the electrons are extracted, whereas $I_0\approx I_T^-$ is the pure projectile current, which approximately equals the target current at full suppression of electron extraction I_T^- (optionally corrected), and (ii) introducing also the collector current (when extracting the emitted electrons) I_C^+, which leads to $\gamma_2=\frac{q}{c}\frac{I_c^+-I_c^-}{I_o}$. When necessary, a small correction, which accounts for the current contribution of electrons emitted from the grid due to backscattered primaries, is applied to the projectile current, making use of the measured current at the grid. Accepted measurements show agreement of both values γ_1 and γ_2 within

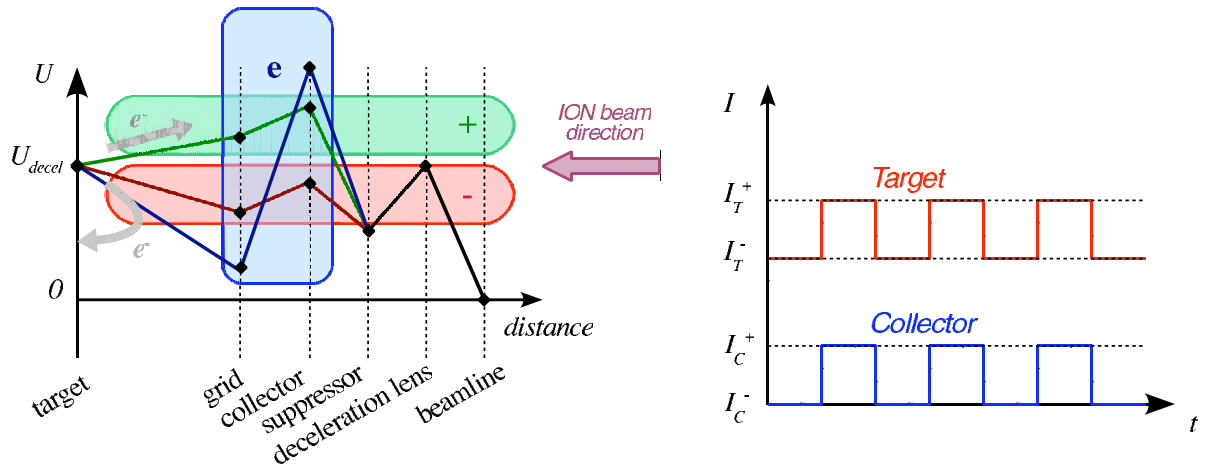

FIG. 2. (Color online) Schematic illustration of the voltage switching states and the corresponding time-dependent electric current at the collector electrode and the target, respectively.

the total estimated statistical error of approximately ±5%. At the very low electron emission yields we expect larger uncertainties due to pickup noise and statistical fluctuations, resulting in an estimated minimum error of 0.02 e^-/ion.

III. RESULTS AND DISCUSSION

A. Energy loss

Figure 3 presents an energy spectrum of 700 eV protons backscattered from one of the Au/B/Si samples. The spectrum is well reproduced by a Monte Carlo simulation using the TRBS code and a proper value for the electronic stopping power (solid line). Note that the TRBS simulations are sensitive to electronic stopping similarly as conventional RBS; changing the stopping power in the simulation by a constant factor essentially leads to an equivalent change of the spectrum width. TRBS accounts for multiple scattering and electronic stopping along the trajectories and thus yields realistic energy spectra of scattered projectiles even at the extremely low energies used in this experiment. Most of the simulations were performed using the "universal" potential with fixed Au layer thickness and the electronic stopping power as an adjustable parameter (by use of a multiplicative correction factor c_s to the SRIM stopping) to optimize the width of the simulated spectrum. For the spectrum shown in Fig. 3, best agreement was obtained for a simulation performed using $S=1.65\times10^{-15}$ eV cm^2 (solid line) corresponding to $c_s=0.33$. The dashed lines in Fig. 3 correspond to simulations performed for electronic stopping values that are larger (smaller) than the optimum value by 18%, showing the high sensitivity of the spectrum width to electronic stopping. This procedure permits to safely deduce the electronic stopping cross section without any influence of multiple scattering.

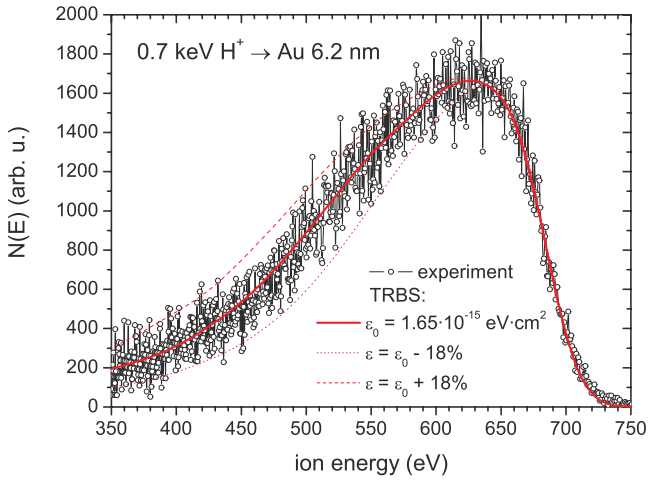

FIG. 3. (Color online) Experimental TOF-LEIS spectra for 700 eV H^+ (1.4 keV H_2^+) ions scattered off the *in situ* deposited Au/B/Si film. The corresponding simulated TRBS spectrum corrected for the stopping cross section is also shown (solid line). Simulations obtained when using an ε value that are larger or smaller than the optimum value ε_0 by 18% are also shown as dashed and dotted lines, respectively.

Figure 4 presents the stopping cross section ε of Au for protons (full circles) and deuterons (full squares) as a function of ion velocity. Our data reveal that for velocities $v<0.18$ a.u., the stopping cross section is proportional to the ion velocity $\varepsilon=Qv$. In the velocity range 0.18 a.u.$\leq v\leq0.6$, the velocity dependence of the stopping cross section can be described as $\varepsilon=c(v-v_{th})$ (dotted line). Here, v_{th} denotes an apparent threshold at ~0.1 a.u. The quantity of interest, however, is $v_0=0.18$ a.u., which represents the threshold for the excitation of the Au $5d$ electrons.[24] At $v>v_0$ an increasing fraction of the $5d$ electrons contributes to electronic stopping, until at $v=0.47$ the $5d$ electrons are expected to be fully active.[24] Consequently, the velocity regime $v<v_0$ corresponds to electronic stopping solely due to the $6s$ electrons, i.e., an electron gas characterized by $r_s=3.02$. For $v>0.47$ a.u., all conduction electrons can be excited. There, $\varepsilon\propto v$ should hold again and a density parameter $r_s=1.49$ a.u. should be adequate.[25]

In Fig. 4, also data from Refs. 9 and 26–28 are shown. Obviously, the different data sets scatter considerably, partly

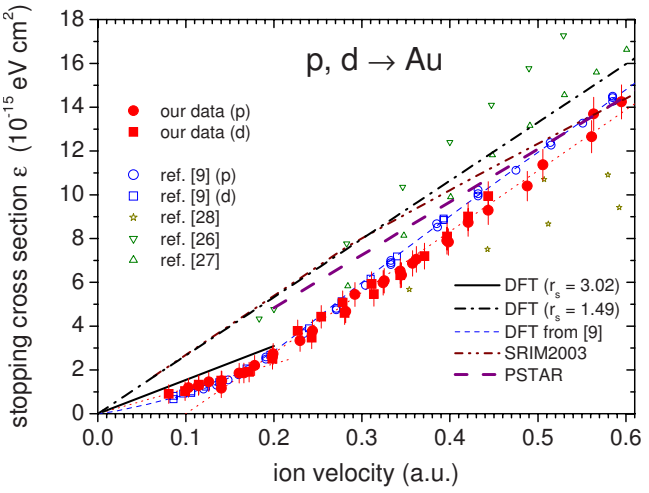

FIG. 4. (Color online) Stopping cross section for hydrogen ions obtained for H_n^+ and D_n^+ with $n=1$, 2, and 3 (circles and squares, respectively) as a function of the ion velocity in a.u. Also shown are data from Refs. 9 and 26–28 and SRIM.

due to enormous experimental difficulties to obtain quantitative information on the stopping cross section for ions below 1 keV/u, partly due to different physical situations. The data from Refs. 26–28 were all measured in transmission using polycrystalline Au films. Note that the absolute values of Refs. 26 and 27 differ only because of different thickness calibrations. No systematic difference is expected between transmission and backscattering experiments through polycrystalline material, since for both geometries the relative contributions of different impact parameters to electronic stopping are expected to be very similar due to strong multiple scattering. For single crystals, however, reduced electronic stopping is expected in channeling compared to a polycrystalline sample of the same material due to more restrictive impact-parameter selection[29] in channeling.

The only data that extend to similarly low velocities as our results are the data from Ref. 9 which were obtained by transmission of slow H ions through Au single crystals. Even these data agree qualitatively very well although they were obtained in channeling geometry in Au(100). A quantitative comparison is not possible for two reasons: first, because of different scattering geometries (channeling vs random) and second, because of different thickness calibrations. In Ref. 9 the foil thickness was calibrated by use of data by Blume *et al.*,[29] which for polycrystals are considerably higher than more recent compilations.[18,30] Nevertheless, for $v<0.18$, our results are higher than the data of Figueroa *et al.*[9] by 17%, while for $v>0.2$ a.u both data sets agree within 10%. Using a common thickness calibration, larger differences would be observed.

Also tabulated are stopping values from SRIM-2003 (Ref. 30) (dash-dot-dotted line) and the electronic stopping database PSTAR (Ref. 18) is included in Fig. 4. At 9 keV our data are identical to PSTAR due to the thickness calibration; at low velocities our data are lower than the tabulated values by up to 50%.

Note that the velocity dependences for protons and deuterons coincide. In other words, there is no isotope effect in stopping of hydrogen ions in gold in the energy range 0.167–5 keV/u, as expected from the binary collision model. The spectra obtained at the same specific energy with different ion species, e.g., 3 keV D^+, 6 keV D_2^+, and 9 keV D_3^+, demonstrate noticeable increase of the spectrum width only for triatomic projectiles (~12% with respect to atomic ions) while for dimers and atomic ions only very minor differences in the spectrum shapes are obtained (~3%–4%). This indicates that our data are hardly influenced by the vicinage effect in electronic stopping.[31] Since backscattering is so unlikely, only at most one particle out of a molecule will be backscattered. Thus, the constituents of a molecular projectile travel individually well separated from each other for the major part of their trajectories. At these low velocities the vicinage effect is expected to be small anyhow since the dwell time $\Delta\tau_d$ of the projectiles in the sample ($\Delta\tau_d = \Delta x/\langle v\rangle$) is large and multiple scattering abolishes further the spatial correlation between the projectiles.

When trying to estimate the accuracy of the resulting stopping cross-section data, the following main contributions to possible systematic errors have to be considered: target thickness, target impurities, and data evaluation. Any systematic error in the absolute value of the PSTAR value at 9 keV will affect our data, with an estimated systematic uncertainty of ±10% (standard deviation). For our *in situ* samples, purity is *a priori* no problem since they are produced in UHV, but also for the *ex situ* sample, bulk impurities are expected to be negligible since Au is a noble metal. Surface impurities do not influence the measurement noticeably in a backscattering experiment.[32] In the data evaluation, a possible systematic uncertainty may be expected from the scattering potential that is not perfectly well known. In order to estimate a possible systematic error arising from the data evaluation, we performed simulations using both the universal potential[33] and the Thomas-Fermi-Molière potential,[34] which resulted in only minor changes in the spectrum shapes. Therefore, possible systematic errors in the stopping power due to the evaluation procedure are expected to be <5%. To conclude, the perfect agreement of experiment and simulation in Fig. 3 gives confidence that the evaluation procedure is stable and the resulting ε values are reliable to within an overall systematic uncertainty of ~10%–15%. The statistical uncertainty is estimated to be ±5% standard deviation for velocities >0.35 a.u.; at velocities below 0.35 a.u., a constant statistical error of $\pm 0.3\times 10^{-15}$ eV cm^2 may be more realistic.

Finally, we want to compare our results to DFT calculations. To this aim, we mimic the 6*s* electrons by an electron gas of adequate density ($r_s=3.02$) and perform a DFT calculation using the friction coefficient from Ref. 35 for this r_s value. The resulting DFT curve is somewhat higher than the experimental data (by 17%) as shown in Fig. 4 (solid line). This may be considered as satisfactory agreement. For the same velocity range, Figueroa *et al.*[9] performed DFT calculations for the same r_s value, but replaced v_F by a relative velocity $v_r \approx 0.75 v_F$ for the electrons (short dashed line). Due to the assumed proportionality of ε to v_F, ε is also reduced by a factor 0.75. On the one hand, the introduction

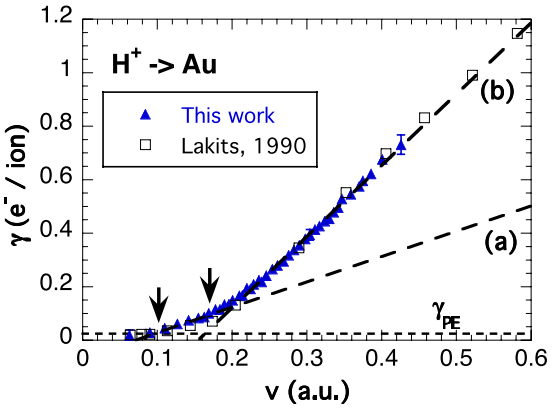

FIG. 5. (Color online) Total electron emission from Au excited by impinging protons. The total number of emitted electrons per incident ion is shown. The dashed lines labeled (a) and (b) indicate linear fits of two distinct regimes in the data set. A horizontal dashed line represents the potential emission contribution γ_{PE} to the total yield. The expected emission thresholds for $6s$ electrons (at around 0.10 a.u.) and $5d$ electrons (at around 0.17 a.u.) are indicated by arrows (cf. text). The statistical error is estimated to $\pm 5\%$ but never smaller than 0.02 and indicated at selected points. For comparison, previous results are included (Refs. 15 and 37).

of $v_r = 0.75 v_F$ abolishes the discrepancy between DFT and their channeling data. On the other hand, the use of a relative velocity smaller than v_F is questionable in the velocity range of interest ($v \ll v_F$), since the exclusion principle limits the interaction to the electrons at the Fermi level.

In the velocity range 0.18 a.u. $< v <$ 0.47 a.u., the data cannot be described in a free-electron picture. The calculation for $r_s = 1.49$ a.u. (dash-dotted line) is expected to be a realistic description of the stopping in the velocity range where all the valence electrons contribute to the stopping process ($v > 0.47$ a.u.). Our experimental data just extend up to $v = 0.6$ a.u., where their absolute value was fixed. An extension of the data toward higher velocities would be required to verify whether it is adequate to describe the gold conduction band as an electron gas with $r_s = 1.49$ a.u. In Ref. 9 the free-electron-gas calculation was modified by introducing a finite minimum-energy transfer for the $5d$ electrons such that the resulting curve perfectly fits the experimental data.

B. Electron emission

Several theoretical descriptions suggest proportionality between the electronic stopping and the total electron emission, respectively,[10] therefore we performed electron emission yield measurements in the same velocity regime as in the case of stopping power in order to be able to compare the obtained results, especially concerning the distinct threshold for the excitation of $5d$ electrons in the stopping power reported above. The results of the electron emission measurements are presented in Fig. 5, which shows an average of multiple independent measurements, each one covering the complete velocity range. For each such experiment, the target was sputter-cleaned in advance.

Because of the comparably small potential energy of the protons, potential electron emission (PE) does not contribute significantly to the total electron emission yield. Using the semiempirical formula given by Kishinevsky[36] $\gamma_{\mathrm{PE}} \approx \frac{0.2}{E_F}(0.8E_{\mathrm{pot}} - 2W)$, with the Fermi-energy E_F around 7.3 eV,[14] the projectile potential energy E_{pot} (13.6 eV), and the work function W of the polycrystalline gold [5.1 eV (Ref. 13)], one can estimate the potential electron emission yield to roughly 0.02 e^-/ion. Using the same parameters for E_F and W in the simple classical threshold model of Eq. (2) leads to a threshold velocity for KE of 0.11 a.u. When introducing the effective mass of the electrons inside the solid, this value slightly shifts to roughly 0.10 a.u. (Ref. 15). Since for the asymmetric H-Au system no significant contributions due to level-promotion are expected, the direct collision excitation mechanism is the predominant contribution for KE.[37]

The classical threshold is indicated in the figure with an arrow; the location along the velocity axis at 0.10 a.u. fits nicely the presented measured data when taking the PE contribution into account. In the projectiles' velocity regime between 0.10 and 0.18 a.u. the yield increases linearly with the projectile velocity, but eventually deviates from this linear behavior above roughly 0.18 a.u. Staying within the simple picture of having (nearly) free electrons of $v < v_F$ which are excited by direct collisions with impinging projectiles, one could estimate the effect of the $5d$ electrons by (i) taking into account their higher effective work function they have to overcome and their at the same time (ii) smaller velocity (energy), which can be accounted for by lowering the effective Fermi energy by the same amount of roughly 2 eV.[14] Of course, this simple description ignores the localized character of the d electrons, which makes a free-electron approximation questionable, but at the same delivers a first estimate for the expected kinematic threshold for these electrons. Inserting the modified values for W and E_F into Eq. (2), one obtains about 0.17 a.u. for the $5d$ threshold, which interestingly matches the location of the kink in the velocity dependent total yield within reasonable limits. The location of this value in Fig. 5 is indicated by an arrow. In this chart, the dashed line labeled (a) would therefore represent the contribution of the $6s$ electrons, whereas above roughly 0.18 a.u. also the $5d$ electrons can be ejected from the sample due to direct collisions with the projectiles. The linear fits, which make also use of previously measured data,[15,37] deliver a location of the transition region where the $5d$ electrons start to contribute of around 0.19 a.u. Eventually, a comparison between the slopes within the two different regimes, one below 0.19 a.u., the other above, leads to a factor 2.86 in between in the case of electron emission, which can be compared to roughly 2.4 in the case of the electronic stopping power.

In summary, we report a clear threshold behavior in the interaction of hydrogen ions with polycrystalline gold in electronic stopping and in ion-induced electron emission. A rather sharp, distinctive threshold velocity of ~0.19 a.u. is observed for specific excitation and emission of $5d$ electrons; below this threshold the projectiles interact exclusively with the $6s$ electrons. The electronic stopping data qualitatively agree with experiments obtained in transmission through single crystals; the electron emission data are in good quan-

titative agreement with semiempirical estimates. From the concordant features observed in electron emission and electronic stopping one can conclude that there is indeed a very close relation between these two processes, even at ion velocities close to the electron emission threshold. It has to be noted, however, that the usually assumed proportionality $\gamma \propto dE/dx$ cannot hold at velocities below the electron emission threshold, where the electronic stopping still is finite.

ACKNOWLEDGMENTS

This work has been supported by Austrian FWF (Projects No. 17449-N02 and No. P16173-N08). D.P. acknowledges financial support due to a DOC foundation by the Austrian Academy of Science.

[1] P. M. Echenique, F. Flores, and R. H. Ritchie, Solid State Phys. **43**, 229 (1990).
[2] M. J. Puska and R. M. Nieminen, Phys. Rev. B **27**, 6121 (1983).
[3] P. M. Echenique, R. M. Nieminen, J. C. Ashley, and R. H. Ritchie, Phys. Rev. A **33**, 897 (1986).
[4] I. Nagy, A. Arnau, and P. M. Echenique, Phys. Rev. A **40**, 987 (1989).
[5] A. Arnau, M. Peñalba, P. M. Echenique, F. Flores, and R. H. Ritchie, Phys. Rev. Lett. **65**, 1024 (1990).
[6] M. Peñalba, A. Arnau, P. M. Echenique, F. Flores, and R. H. Ritchie, Europhys. Lett. **19**, 45 (1992).
[7] S. N. Markin, Ph.D. thesis, J. K. University Linz, 2007.
[8] S. P. Chenakin, S. N. Markin, E. Steinbauer, M. Draxler, and P. Bauer, Nucl. Instrum. Methods Phys. Res. B **249**, 58 (2006).
[9] E. A. Figueroa, E. D. Cantero, J. C. Eckardt, G. H. Lantschner, J. E. Valdés, and N. R. Arista, Phys. Rev. A **75**, 010901 (2007).
[10] D. Hasselkamp, in *Particle Induced Electron Emission II*, edited by G. Höhler (Springer, Heidelberg, 1992), Vol. 123, p. 1.
[11] J. Burgdörfer, C. Lemell, F. Aumayr, and H. P. Winter, in *Slow Heavy-Particle Induced Electron Emission From Solid Surfaces*, Springer Tracts in Modern Physics Vol. 225, edited by H. P. Winter and J. Burgdörfer (Springer, New York, 2007), Chaps. 1, 3, and 4.
[12] R. A. Baragiola, E. V. Alonso, and A. Oliva Florio, Phys. Rev. B **19**, 121 (1979).
[13] D. E. Eastman, Phys. Rev. B **2**, 1 (1970).
[14] I. Mertig, E. Mrosan, U. Fleck, and H. Wonn, J. Phys. F: Met. Phys. **10**, 407 (1980).
[15] G. Lakits, F. Aumayr, M. Heim, and H. Winter, Phys. Rev. A **42**, 5780 (1990).
[16] J. Lörincik, Z. Sroubek, H. Eder, F. Aumayr, and H. P. Winter, Phys. Rev. B **62**, 16116 (2000).
[17] M. Draxler, S. N. Markin, S. N. Ermolov, K. Schmid, C. Hesch, R. Gruber, A. Poschacher, M. Bergsmann, and P. Bauer, Vacuum **73**, 39 (2004).
[18] M. J. Berger, J. S. Coursey, and M. A. Zucker, ESTAR, PSTAR, and ASTAR: Computer Programs for Calculating Stopping-Power and Range Tables for Electrons, Protons, and Helium Ions (version 1.2.2). [Online] available: http://physics.nist.gov/Star. National Institute of Standards and Technology, Gaithersburg, MD, 2000.
[19] D. Primetzhofer, S. N. Markin, P. Zeppenfeld, P. Bauer, S. Prusa, M. Kolibal, and T. Sikola, Appl. Phys. Lett. **92**, 011929 (2008).
[20] http://www.veeco.com/
[21] J. P. Biersack, E. Steinbauer, and P. Bauer, Nucl. Instrum. Methods Phys. Res. B **61**, 77 (1991).
[22] E. Galutschek, R. Trassl, E. Salzborn, F. Aumayr, and H. P. Winter, J. Phys.: Conf. Ser. **58**, 395 (2007).
[23] S. Cernusca, H. P. Winter, F. Aumayr, A. Qayyum, W. Schustereder, C. Mair, P. Scheier, and T. D. Mark, J. Mass Spectrom. **223-224**, 21 (2003).
[24] J. E. Valdés, J. C. Eckardt, G. H. Lantschner, and N. R. Arista, Phys. Rev. A **49**, 1083 (1994).
[25] D. Isaacson, *New York University, University Document No. 02698* (National Auxiliary, New York, 1975).
[26] G. Martínez-Tamayo, J. C. Eckardt, G. H. Lantschner, and N. R. Arista, Phys. Rev. A **54**, 3131 (1996).
[27] J. E. Valdés, C. Agurto, F. Ortega, P. Vargas, R. Labbé, and N. R. Arista, Nucl. Instrum. Methods Phys. Res. B **164**, 268 (2000).
[28] A. Nomura and S. Kiyono, J. Phys. D **8**, 1551 (1975).
[29] R. Blume, W. Eckstein, H. Verbeek, and K. Reichelt, Nucl. Instrum. Methods Phys. Res. **194**, 67 (1982).
[30] J. F. Ziegler, The Stopping and Range of Ions in Matter, SRIM-2003 (version 2003.26). [Online] Available: http://srim.org.
[31] J. E. Valdés, C. Parra, J. Díaz-Valdés, C. D. Denton, C. Agurto, F. Ortega, N. R. Arista, and P. Vargas, Phys. Rev. A **68**, 064901 (2003).
[32] P. Bauer, Nucl. Instrum. Methods Phys. Res. B **27**, 301 (1987).
[33] J. F. Ziegler, J. P. Biersack, and U. Littmark, *The Stopping and Range of Ions in Solids* (Pergamon, New York, 1985), Vol. 1.
[34] G. Moliere, Z. Naturforsch. A **2A**, 133 (1974).
[35] M. J. Puska and R. M. Nieminen, Phys. Rev. B **27**, 6121 (1983).
[36] L. M. Kishinevsky, Radiat. Eff. **19**, 23 (1973).
[37] G. Lakits, A. Arnau, and H. Winter, Phys. Rev. B **42**, 15 (1990).